An improved method for direct incident solar radiation calculation from hourly solar insolation data in building energy simulation

Jingjing An[a,b*], Da Yan[c*], Siyue Guo[c,d], Yan Gao[a], Jinqing Peng[e], Tianzhen Hong[f]

[a] *Beijing Key Lab of HVAC, School of Environment and Energy Engineering, Beijing University of Civil Engineering and Architecture, Beijing 100044, China*

[b] *Beijing Advanced Innovation Center for Future Urban Design, Beijing University of Civil Engineering and Architecture, Beijing 100044, China*

[c] *Building Energy Research Center, Tsinghua University, Beijing 100084, China*

[d] *Institute of Energy, Environment and Economy, Tsinghua University, Beijing 100084, China*

[e] *College of Civil Engineering, Hunan University, Changsha 410082, China*

[f] *Building Technology and Urban Systems Division, Lawrence Berkeley National Laboratory, Berkeley, USA*

[*] *Corresponding author, E-mail address: yanda@tsinghua.edu.cn, anjingjing@bucea.edu.cn*

Abstract:

Solar radiation considerably influences the energy consumption of buildings and the power production of building integrated photovoltaic (BIPV) systems. Hourly solar insolation (Wh/m^2), represented as the amount of solar irradiance collected on the ground during a 1-h period, is the most common solar radiation data available and widely used in weather files applied in building energy modeling programs (BEMPs). Because the solar beam and position vary over time, the use of hourly insolation data as the input might result in errors in the estimation of the direct incident solar radiation on a particular surface. In this study, methods used in BEMPs for direct incident solar radiation calculations are first analyzed, and an improved method adopting a new algorithm for estimating the solar irradiance is proposed. The algorithm assumes that the solar irradiance changes linearly within a 1-h period and can be estimated based on the solar irradiance at the half clock and slope. The collected direct normal solar irradiance data of 2016 from eight solar radiation stations in China were used to demonstrate the proposed method and evaluate its performance by comparing the results with those from three conventional methods used in BEMPs along with the ground truth measurements. In addition, in this study, factors affecting the accuracy of the calculation results are explored. The results of the estimated direct incident solar radiation show that the proposed method achieves the best accuracy, followed by the methods used in DOE-2, EnergyPlus, and DeST. The proposed method guarantees that the hourly direct solar insolation will remain the same and reflects the variation in the direct solar irradiance across a 1-h time frame. The proposed method can be adopted in BEMPs to improve the accuracy of the solar radiation calculation, thereby improving the accuracy of the simulated building performance and the BIPV production.

Keywords:

Direct incident solar radiation on surfaces; calculation method; hourly solar insolation; building energy simulation; BIPV systems

1. Introduction

Solar radiation plays a significant role in building energy consumption. The building environment and building thermal energy consumption are responsive to the solar radiation conditions, particularly for buildings with glazed envelopes or large windows [1,2]. Solar radiation penetrating into rooms through windows can directly impact the indoor thermal environment. It can also increase the outside surface temperature of the envelope, thereby affecting the indoor environment and cooling/heating loads. Solar radiation is regarded as the main contributor to heat gains in buildings, particularly in residential buildings, where the internal gains are extremely low [3]. The US Department of Energy reported that solar heat gain from windows in cooling-dominated climates has a significant energy impact on both residential and commercial buildings [4]. Chen et al. [5] found that approximately 20%–30% of the cooling load in buildings is from external windows in summer in Northern China, whereas the proportion is even higher in Southern China. Yin et al. [6] analyzed the cooling loads of two commercial buildings equipped with a solar window film in Shanghai, China, and found that the building loads from solar radiation through windows account for 44% and 47% of the total loads, respectively. Therefore, solar radiation is a key meteorological parameter for building heating/cooling load estimation. In addition, solar radiation is also related to daylighting. The utilization of daylighting can be beneficial to building energy conservation and a comfortable indoor environment [7]. A better understanding of solar radiation may result in successful building design and air-conditioning system sizing [8].

Solar photovoltaic technology is one of the best ways to utilize solar power [9]. With increased building energy consumption, an increasing demand for renewable energy exists in buildings. Thus, building integrated photovoltaic (BIPV) systems have been applied to numerous applications in recent years [10]. Solar radiation is the key factor determining the electricity production of BIPV systems. To make better use of BIPV systems, the variation and maximum utilization of solar radiation incident on solar photovoltaic (PV) panels are valuable in the design stage [11]. Solar radiation data are necessary for evaluating the profitability in installing a BIPV system [12]. However, solar radiation received by a solar PV panel is affected by its orientation and tilt angle, which vary from each other, and the measured data are extremely limited [13]. As a consequence, the calculation method regarding solar radiation incident on a panel surface is worth studying.

Solar radiation data are necessary for calculating the solar radiation incident on a tilted surface. Most countries have their own meteorological radiation stations for monitoring solar radiation data. Slater [14] gathered the solar radiation data from over 4,000 stations, covering much of the continental United States as well as portions of Alberta and British Columbia, Canada. A total of 22 out of 92 weather stations are equipped with sensors to monitor solar radiation data in South Korea [15]. In China, there are 122 stations recording solar radiation data, which are divided into three levels based on the number of measured parameters [16,17]. However, owing to a limited number of stations, the measured solar radiation data are insufficient in many parts of the world. Therefore, numerous researchers have utilized reliable solar models with ground or satellite-based datasets to generate solar radiation data under a high spatial resolution. Janjai et al. [18] compared the estimation of the monthly average daily solar radiation from long-term satellite data with the data measured by meteorological stations throughout Cambodia. It was demonstrated that accurate

estimation results can be obtained from satellite data with a root mean square difference of only 6.4%. Solar radiation models can be divided into three types: regression, mechanistic, and state-of-the-art approaches. Cloud-cover radiation model [19] and Zhang and Huang's model [20] are regression models of hourly solar radiation prediction developed from historical solar radiation data and other related meteorological data such as the amount of cloud cover. To overcome the limitation of regression models, Kambezidis and Psiloglou [21] proposed a meteorological radiation model, forecasting the global solar radiation for clear and overcast skies by calculating the conditions of the atmospheric constituents that cause the absorption and scattering of extraterrestrial radiation on the way to the ground. Wild et al. [22] utilized the solar radiation data generated by climate models in IPCC-AR4/CMIP3 to analyze the global dimming and brightening. In recent years, machine learning algorithms have been widely used in solar radiation prediction in sites where measured data are deficient. A popular approach for solar radiation prediction is the artificial neural network (ANN). Huang et al. [23] developed a hybrid auto regression and dynamical system model to predict the hourly global solar radiation in Australia. In addition, the results show that the ANN method can achieve a more accurate solar radiation protection compared with conventional methods [24]. The support vector machine model was also adopted in a study on global solar radiation prediction [25].

Numerous solar radiation databases based on either observations or simulated data have been established in many countries [18,26–28]. For instance, the National Solar Radiation Data Base (NSRDB) has been widely used by an increasing number of researchers and the industry since 1994. NSRDB provides publicly open data on solar radiation and meteorological data over the United States and regions of the surrounding countries [29]. In addition, typical meteorological year (TMY) data were developed from NSRDB for the building analysis, and the forecast and comparison of the solar system performance, mainly in the United States and Canada. The latest version is TMY 3 based on meteorological data from 1991–2005 [30,31]. Typical weather files have been established in many countries based on approximately 20–30 years of historical data with different variables and selection methods [32]. For instance, the American Society of Heating, Refrigerating, and Air-Conditioning Engineers (ASHRAE) proposed the International Weather for Energy Calculations Version 2.0 (IWEC2) in 3012 stations outside the United States and Canada [33–35]. The Test Reference Year (TRY) was developed by the Chartered Institution of Building Services Engineers (CIBSE) in 14 stations in the United Kingdom [36]. In addition, the China Meteorological Bureau and Tsinghua University built their own typical weather files called Chinese Standard Weather Data (CSWD) in 270 stations in China [37].

However, the most available solar radiation data found in such datasets are hourly insolation data. The hourly solar insolation is the total amount of solar radiation collected on the ground within 1 h, the unit of which is Wh/m^2. Instantaneous solar irradiance, with a unit of W/m^2, is difficult to obtain. The 122 meteorological radiation stations in China can only report hourly solar insolation data. There are only seven baseline surface radiation stations in China, as a part of the Baseline Surface Radiation Network (BSRN), that can provide solar irradiance on the ground on a minute by minute basis. BSRN was created in 1992 by the World Climate Research Programme to provide accurate irradiances with a high temporal resolution globally [38].

BEMPs, such as DOE-2 [39], DeST [40], and EnergyPlus [41], usually use the hourly solar insolation (Wh/m^2) in weather files, which represent the total amount of irradiance within 1 h. As shown in Figure 1, different BEMPs use their own algorithms to estimate the solar irradiance (W/m^2)

from hourly solar insolation in weather files, and the estimated solar irradiance should then be applied to calculate the solar radiation incident on different surfaces [42]. However, solar radiation varies over time, and it has a significant variation even within a 1-h time frame. Using the hourly solar insolation as input for the calculation of the solar radiation on a tilted surface might cause errors compared with the actual value, which is a key bottleneck that should be discussed in this study. Particularly for direct solar radiation, its corresponding solar position also changes over time, which can further impact the amount of solar radiation falling on a tilted surface.

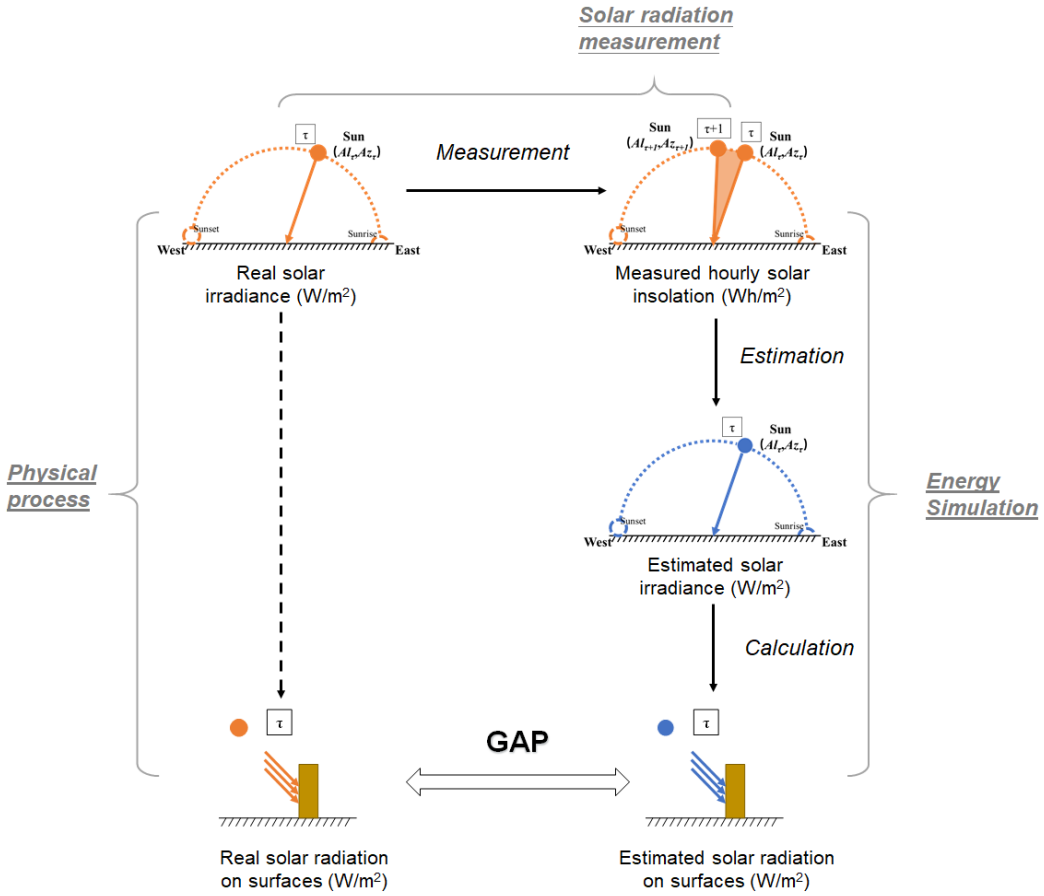

Figure 1 Key bottleneck in energy simulation of direct solar radiation on a surface

Hourly solar insolation data are the most commonly available data used in modeling the building energy consumption and electric energy production of BIPV systems[43]. Using hourly solar insolation data can lead to a gap between the estimated direct solar radiation incident on the surfaces and the actual value. As a result, it is essential to compare different calculation methods when using hourly solar insolation data as the input. McDowell and Kummert [42] and Zhu et al. [44] compared the solar radiation calculation from hourly weather data in different BEMPs separately, and found that the different methods impact the simulation results significantly. However, they only carried out a comparison among the simulation results of different BEMPs, instead of conducting a comparison between simulations and the actual instantaneous values. In addition, McDowell et al. .[45] proposed an improved method and compared it with EnergyPlus and TRNSYS 17 based on measured solar irradiance data in minutes in three cities in the United States. They mainly focused on the impacts of different methods on direct normal solar irradiance instead of direct incident solar radiation.

In this study, the calculation methods for direct incident solar radiation calculations used in BEMPs are first analyzed, based upon which an improved method for a direct incident solar radiation calculation is proposed. Based on the collected direct normal solar irradiance (DNSG) data of 2016 from eight radiation stations in China, the proposed method along with three conventional methods were compared and analyzed. In conclusion, we seek to generate knowledge regarding the method for achieving a direct incident solar radiation calculation, thereby contributing to more accurate estimation results from hourly DNSI data.

2. Methodology

2.1. Overview

The overall methodology of this study is shown in Figure 2. In this study, we aimed to improve the present calculation methods used in BEMPs. This study contains four steps: data collection, method development, a case study, and a sensitivity analysis. First, we collected DNSG data from eight radiation stations in China for the year 2016 from the China Meteorological Administration. We then summarized the advantages and disadvantages of the direct incident solar radiation calculation methods applied to three conventional BEMPs (i.e., DOE-2, EnergyPlus, and DeST), based upon which a method was proposed. Third, to evaluate the proposed method for determining the direct incident solar radiation, we compared the estimated direct solar radiation on tilted surfaces obtained by the proposed method and the methods applied in the three BEMPs from hourly DNSI data with the ground truth, which is calculated directly through the DNSG data. Fourth, we further explored the impacts of different factors on the estimation results. Three influencing factors, namely, an estimation algorithm for the solar irradiance, the timestep, and the time point for the solar position, were analyzed through a sensitivity analysis. Finally, we summarize the findings and suggestions for direct incident solar radiation calculations. This study was carried out using MATLAB software [46].

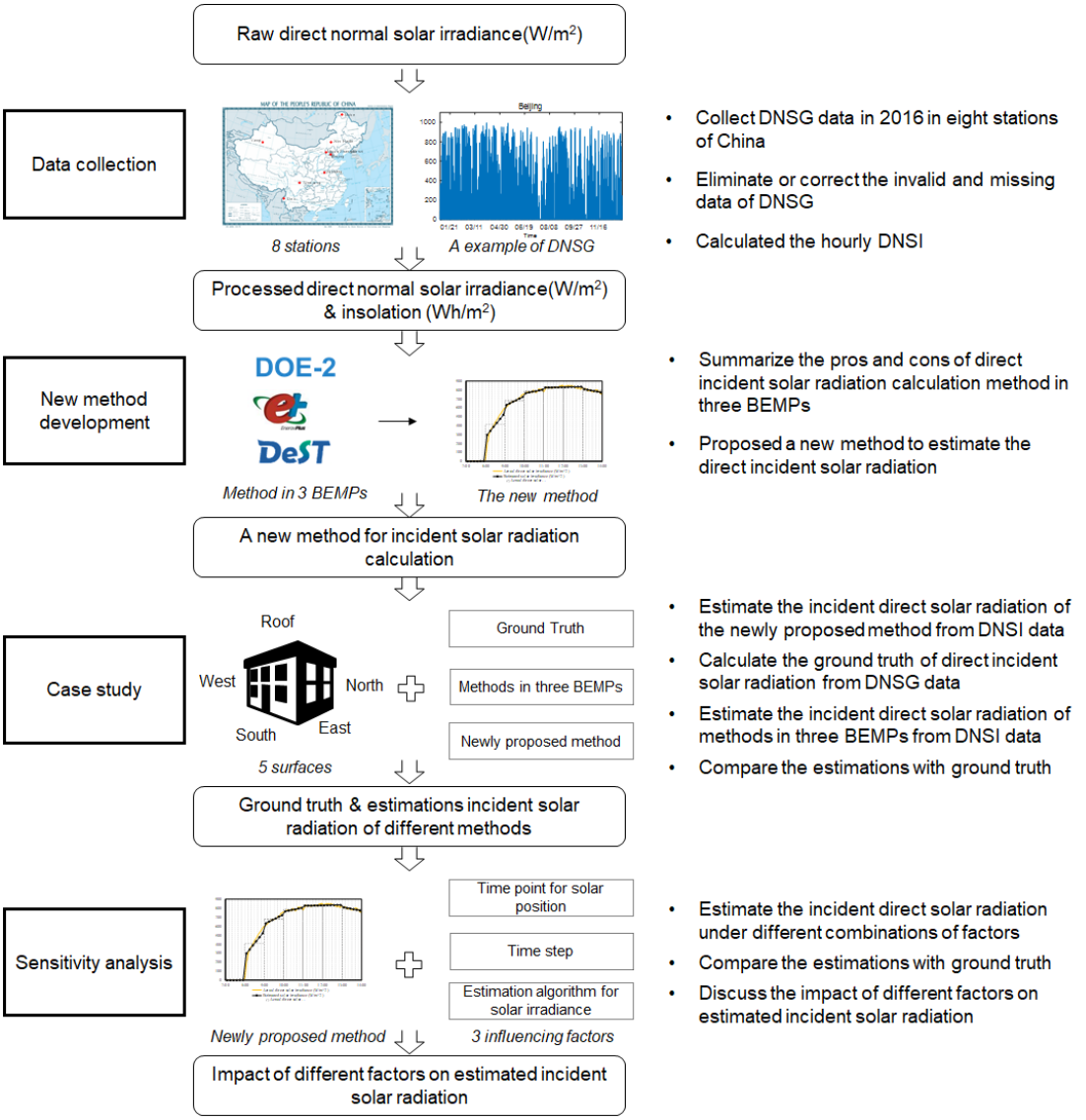

Figure 2 Overall methodology of the present study

2.2. Data collection

Because the different latitudes of various cities have a significant influence on direct incident solar radiation, we selected eight cities in China to discuss the calculation methods, including all BSRN stations throughout China, and Beijing station. The eight stations applied are all Chinese solar radiation stations that can supply solar irradiance data in minutes. Detailed information regarding the selected radiation stations is summarized in Table 1. These cities are located in different climate zones and have diverse latitudes over a large span (i.e., 25°07′N–5 3°47′N). We collected the DNSG data of 2016 from the China Meteorological Administration.

Owing to some invalid or missing data, we carried out a data cleaning prior to the analysis, the basic principles of which are as follows: 1) We eliminated those days (e.g., 6 days from 366 days in Beijing) in which more than one-third of the data are invalid or missing. 2) For the data that were continuously missing or invalid for over a 1-h period, we replaced them with data from the same time on an adjacent day; when this was impossible, we corrected the missing or invalid data using

a linear interpolation between the two known values. The lengths of the valid data after preprocessing are also shown in Table 1.

Table 1 Summary of selected radiation stations

No.	City	Province	Climate Zone	Latitude	Longitude	Valid days
1	Beijing	Beijing	Cold zone	39°48′N	116°28′E	361 days
2	Mohe	Heilongjiang	Severe cold zone	53°47′N	122°37′E	64 days
3	Yanqi	Xinjiang	Cold zone	42°08′N	86°57′E	349 days
4	Xilin Haote	Inner Mongolia	Severe cold zone	43°95′N	116°07′E	350 days
5	Miyun	Beijing	Cold zone	40°65′N	117°12′E	366 days
6	Wenjiang	Sichuan	Hot summer and cold winter zone	30°07′N	103°83′E	365 days
7	Dali	Yunnan	Temperate zone	25°07′N	100°18′E	94 days
8	Xuchang	Henan	Cold zone	34°02′N	113°85′E	366 days

The processed data of eight stations from 2016 are shown in Figure 3. As indicated in the figure, after data processing, 1) Mohe and Dali lack solar data for a long period owing to the poor quality of the collected data, 2) Yanqi, Xilin Haote, and Xuchang have valid long-term solar data from 2016; however, the solar data are often equal to zero, particularly in Yanqi, which might be caused by a failure of the monitoring devices, and 3) Beijing, Miyun, and Wenjiang have long-term and high-quality solar data. We calculated the DNSI data from the processed DNSG as inputs for the calculation methods used in the BEMPs.

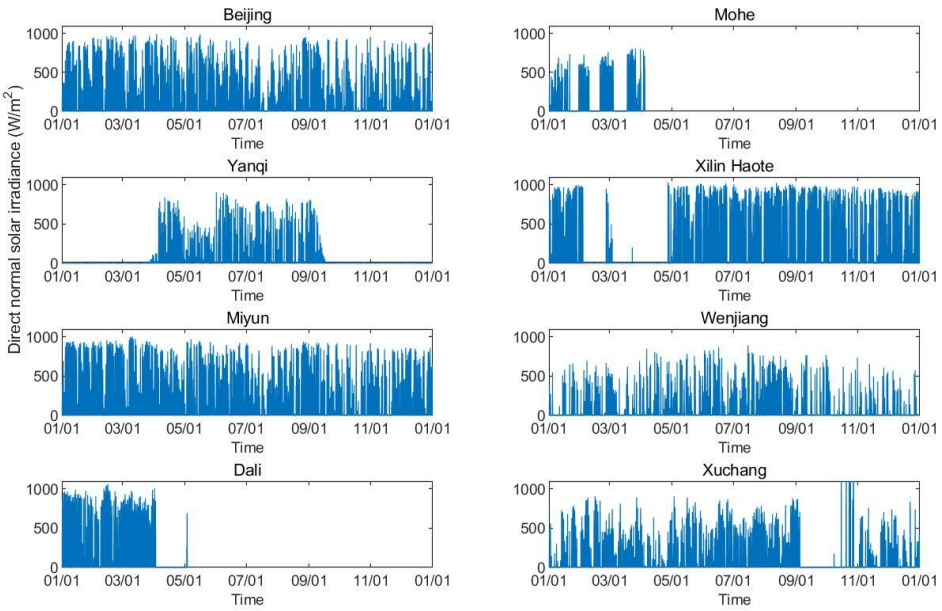

Figure 3 DNSG of eight stations in 2016

2.3. Development of proposed method

2.3.1. Three conventional methods used in BEMPs

We compared the calculation methods of direct solar radiation adopted by DOE-2, EnergyPlus, and DeST in this study, which are certified as qualified software for calculating commercial building tax deductions by the U.S. Department of Energy, and are the most widely used programs around the world. Zhu et al. [44] compared the modeling assumptions and simplifications for calculating the direct solar radiation on surfaces used in these three popular building energy modeling programs. There is no difference between EnergyPlus and DOE-2 in solar calculation if EnergyPlus runs at an hourly timestep. Therefore, the direct solar radiation method in EnergyPlus refers to its method at subhourly timesteps in this study.

A comparison of the direct solar radiation methods for the three BEMPs on a typical day is shown in Figure 4 (the orange vertical line represents sunrise). As the most significant difference in the direct solar radiation calculations, the three BEMPs have different estimation algorithms for solar irradiance. With these programs, the solar radiation data in the weather files are in the unit of Wh/m^2, which represent the total amount of irradiance within a 1-h period. For DOE-2 and DeST, the solar irradiance is considered as a constant within a 1-h time frame, the value of which is equal to the input hourly insolation. By contrast, EnergyPlus assumes that the solar irradiance at the midpoint of 1 h is equal to the average value, which is the same value as in the hourly insolation, and the sub-hourly values are obtained through a linear interpolation. There are also some other differences among these programs. With DOE-2 and DeST, the direct incident solar radiation is calculated every hour, whereas EnergyPlus calculates the direct incident solar radiation every 10 min. In addition, the three programs use different time points for the solar position calculations (the black points in Figure 4 represent the time points for solar position at each timestep), namely, the middle point is used by DOE-2, the beginning point is applied by DeST, and the endpoint is used by EnergyPlus. The sunrise usually appears at sometime within one hour, such as 7:31 for the day shown in Figure 4. According to the solar position calculation methods in BEMPs, the sun sometimes is below the horizon line on the sunrise hour. For instance, as DeST uses the beginning point for solar position, the sun is not up during 7:00-8:00 yet for the day shown in Figure 4.

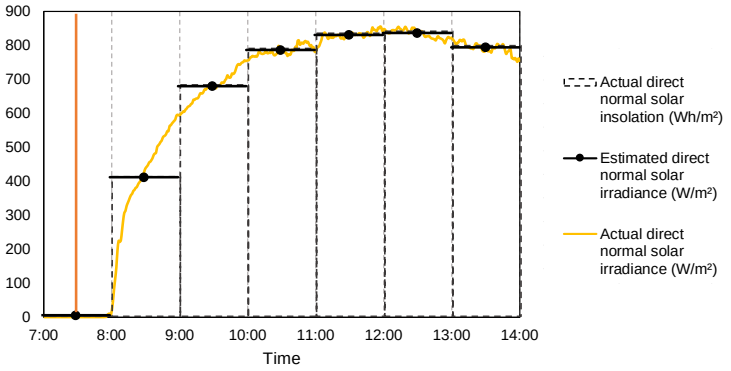

a) DOE-2

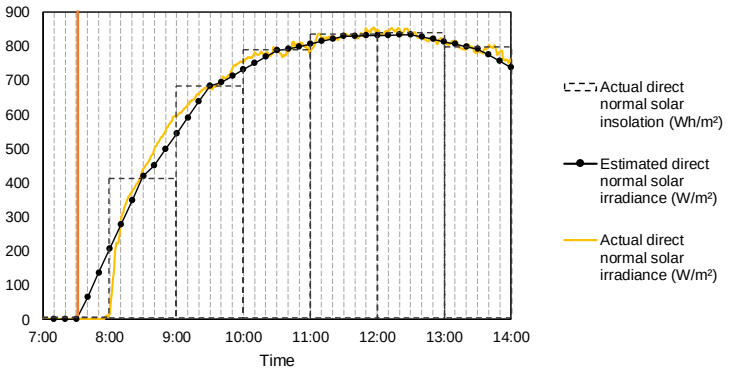

b) EnergyPlus

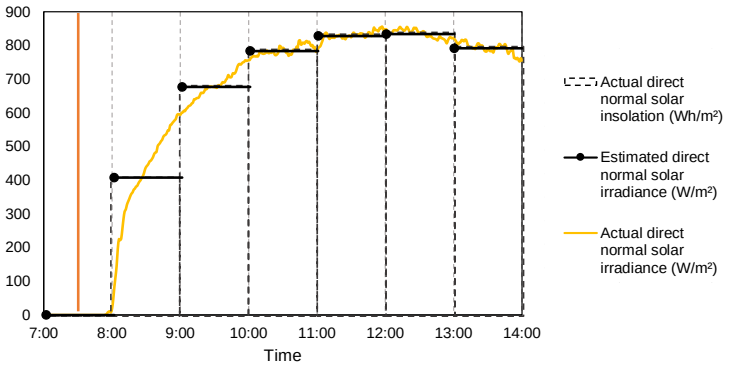

c) DeST

Figure 4 Comparison of direct solar radiation calculation methods for the three BEMPs for a typical day (January 06, 2016 in Beijing)

In Figure 4, the yellow line represents the actual DNSG of a typical day, which fluctuates significantly within a 1-h time frame, particularly a few hours after sunrise and before sunset. The methods adopted by DOE-2 and DeST cannot reflect the actual variation in the DSNG very well. EnergyPlus performs much better by contrast, although the total amount of estimated DNSG within a 1-h period is not equal to the actual DNSI. As shown in Figure 5, the estimated DNSI values are higher than the ground truth at 7:00, 16:00, and 17:00, and lower at all other times.

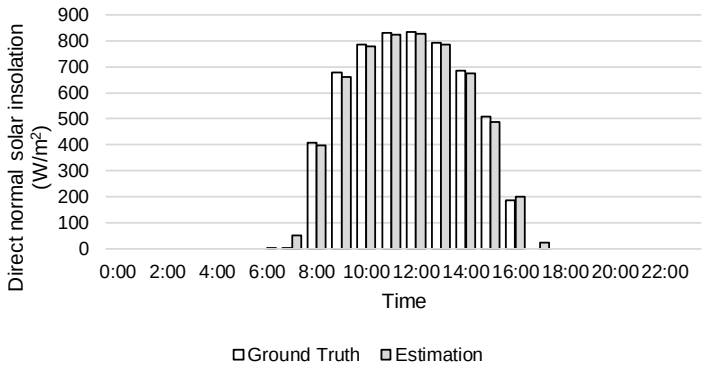

Figure 5 Actual and estimated (by EnergyPlus) DNSI on January 06, 2016 in Beijing

2.3.2. Proposed method

The DOE-2 and DeST assume that the solar irradiance remains constant within a 1-h period, which we call “zero-order interpolation”, and which ignores the variation in solar irradiance within a 1-h time frame, resulting in an estimation error of direct incident solar radiation. By contrast, EnergyPlus uses a first-order interpolation to estimate the DNSG. The DNSG at the half clock is considered to be equal to the average irradiance, and EnergyPlus uses a linear interpolation to connect the solar irradiances at the half-hour clock time, which results in a piecewise-linear profile of the solar irradiances, which does not ensure that the integrated hourly values will match the original data (Figure 5b). In conclusion, there are some disadvantages with these two algorithms for the estimation of the DNSG.

Therefore, we propose a method using a new algorithm to estimate the solar irradiance (Figure 6). Note that the orange vertical line in Figure 6 represents sunrise. This algorithm assumes that the solar irradiance changes linearly within 1 h. The proposed algorithm treats the input hourly solar insolation as the instantaneous solar irradiance at the half clock, and the slope is estimated based on the solar insolation values during the last hour, present hour, and next hour. The solar irradiances can be estimated based on the solar irradiance at the half clock along with the slope of each hour, which keeps the hourly integrated values constant but results in a saw-tooth profile (Figure 6).

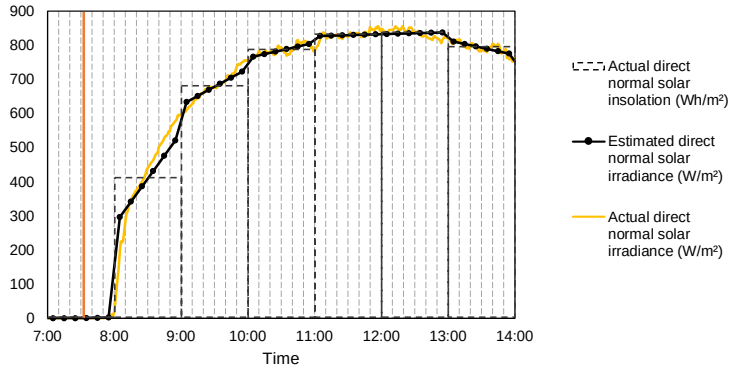

Figure 6 Proposed method for solar irradiance estimation during a 1-day period (Jan. 06, 2016 in Beijing)

The proposed method contains the following steps:

(1) Calculating time of sunrise, solar noon and sunset. Then adjusting the start-time and end-time of every hour for sunrise and sunset. The midpoint of every hour is equal to the average of the start-time and end-time.

(2) Calculating the instantaneous solar irradiance at midpoint of every hour using the following formula:

$$SG_{\mathrm{mid},i} = SI_i / (t_{end,i} - t_{start,i}) \quad (1)$$

where i represents the present hour, t_{end} and t_{start} represent the start-time and end-time of every hour,

SG_{mid} is the instantaneous solar irradiance at midpoint in W/m^2, and SI is the hourly solar insolation in Wh/m^2.

(3) For normal hours between sunrise and sunset, we calculated the slope in a 1-h period using the following formula:

$$SLOPE_i = \begin{cases} \min\left(\frac{SG_{mid,i}-SG_{mid,i-1}}{t_{mid,i}-t_{mid,i-1}}, \frac{SG_{mid,i+1}-SG_{mid,i}}{t_{mid,i+1}-t_{mid,i}}\right) & SG_{mid,i-1} \le SG_{mid,i} \le SG_{mid,i+1} \\ \max\left(\frac{SG_{mid,i}-SG_{mid,i-1}}{t_{mid,i}-t_{mid,i-1}}, \frac{SG_{mid,i+1}-SG_{mid,i}}{t_{mid,i+1}-t_{mid,i}}\right) & SG_{mid,i-1} > SG_{mid,i} > SG_{mid,i+1} \\ -1\times\min\left(\left|\frac{SG_{mid,i}-SG_{mid,i-1}}{t_{mid,i}-t_{mid,i-1}}\right|, \left|\frac{SG_{mid,i+1}-SG_{mid,i}}{t_{mid,i+1}-t_{mid,i}}\right|, \left|\frac{2SG_{mid,i}}{t_{end,i}-t_{start,i}}\right|\right) & else, when \quad t_{mid,i} \le t_{solarnoon} \\ \min\left(\left|\frac{SG_{mid,i}-SG_{mid,i-1}}{t_{mid,i}-t_{mid,i-1}}\right|, \left|\frac{SG_{mid,i+1}-SG_{mid,i}}{t_{mid,i+1}-t_{mid,i}}\right|, \left|\frac{2SG_{mid,i}}{t_{end,i}-t_{start,i}}\right|\right) & else, when \quad t_{mid,i} > t_{solarnoon} \end{cases} \quad (2)$$

where *i-1, i, i+1* represent the last hour, present hour, and next hour, t_{mid} represents the midpoint of every hour, $t_{solarnoon}$ is the time of solar noon, and *SLOPE* is the slope of solar irradiance profile within 1 h.

The proposed method can ensure that the amount of estimated DNSG is equal to the initial insolation, and reflect the variation in irradiance across the hour. However, there might be a gap in the estimated irradiance between the end of the last hour and the beginning of this current hour, that is, the solar irradiance may change discontinuously. Therefore, we used the above formula of slope to minimize the gap between two adjacent hours.

(4) For the sunrise hour, we calculated the slope in a 1-h period using the following formula:

$$SLOPE_i = \begin{cases} \frac{2SG_{mid,i}}{t_{end,i}-t_{start,i}} & SG_{mid,i+1}-(t_{mid,i+1}-t_{start,i+1})SLOPE_{i+1} \le SG_{mid,i}, or \\ & SG_{mid,i+1}-(t_{mid,i+1}-t_{start,i+1})SLOPE_{i+1} \ge 2SG_{mid,i} \\ \frac{SG_{mid,i+1}-(t_{mid,i+1}-t_{start,i+1})SLOPE_{i+1}-SG_{mid,i}}{t_{end,i}-t_{mid,i}} & SG_{mid,i} < SG_{mid,i+1}-(t_{mid,i+1}-t_{start,i+1})SLOPE_{i+1} < 2SG_{mid,i} \end{cases} \quad (3)$$

For the sunset hour, we calculated the slope in a 1-h period using the following formula:

$$SLOPE_i = \begin{cases} -\frac{2SG_{mid,i}}{t_{end,i}-t_{start,i}} & SG_{mid,i\text{-}1}+(t_{end,i-1}-t_{mid,i-1})SLOPE_{i-1} \le SG_{mid,i}, or \\ & SG_{mid,i\text{-}1}+(t_{end,i-1}-t_{mid,i-1})SLOPE_{i-1} \ge 2SG_{mid,i} \\ \frac{SG_{mid,i}-(SG_{mid,i\text{-}1}+(t_{end,i-1}-t_{mid,i-1})SLOPE_{i-1})}{t_{mid,i}-t_{start,i}} & SG_{mid,i} < SG_{mid,i\text{-}1}+(t_{end,i-1}-t_{mid,i-1})SLOPE_{i-1} < 2SG_{mid,i} \end{cases} \quad (4)$$

(5) The solar irradiances can be estimated based on the solar irradiance at midpoint along with the slope of each hour. 10-min timestep and the middle of each timestep for the solar position are used to calculate the direct incident solar radiation on different surfaces.

2.4. Case study

To evaluate the proposed method, we demonstrated its application in eight cities in China to obtain the estimated direct incident solar radiation on tilted surfaces, and compared the results using estimations of three conventional methods and the ground truth when applying the approach shown in Figure 7.

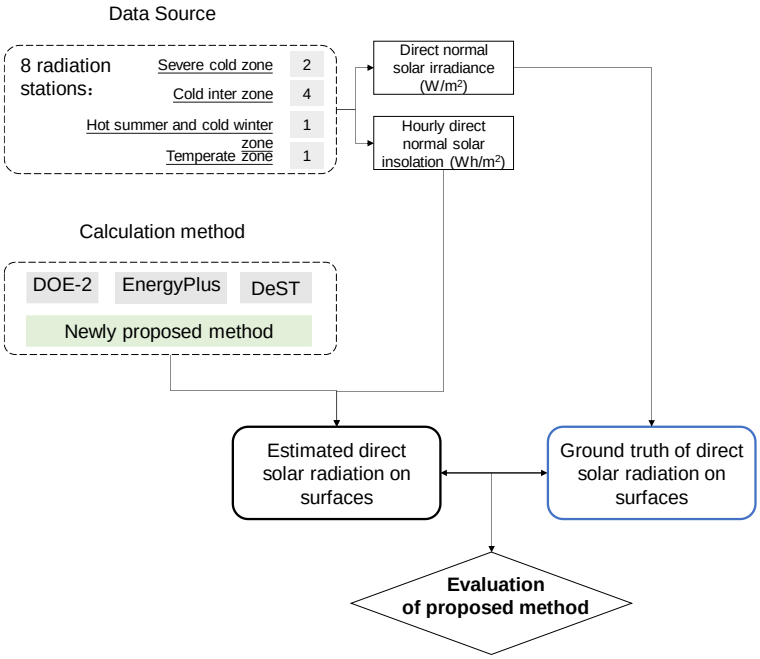

Figure 7 Technical approach of the case study

As mentioned, the DNSG data based on the minute and hourly DNSI data from 2016 were gathered from eight radiation stations throughout China. The DNSG data were recorded in minutes and can be directly used to calculate the direct solar radiation incident on tilted surfaces, which we regard as the ground truth in this study. In addition, four methods (Table 2) were first used to estimate the DNSGs based on the DNSI data, and then to calculate the direct incident solar radiation on the surfaces. In this study, we mainly calculated the solar radiation incident on five surfaces with different angles as examples, namely, a vertical east-facing surface, a vertical west-facing surface, a vertical south-facing surface, a vertical north-facing surface, and a horizontal surface.

Table 2 Summary of various calculation methods

	Estimation of solar irradiance	Timestep	Time point for solar position
DOE-2	Constant within every timestep (0-order interpolation)	1 hour	The middle of every timestep
EnergyPlus	Linear between two adjacent half clocks (1-order interpolation)	10 min	The end of every timestep
DeST	Constant within every timestep (0-order interpolation)	1 hour	The beginning of every timestep
Proposed method	Linear within every timestep (Saw-tooth algorithm)	10 min	The middle of every timestep

The DNSG can be converted into the incident radiation on a tilted surface, based on the geometrical relationship between the receiving surface and the surface perpendicular to the sun's rays [26]. The calculation process is presented as follows. The position of the sun is defined by its altitude (Al) and azimuth (Az), as shown in Figure 8. In this study, the solar azimuth angle is clockwise from due north, and thus east is 90°, south is 180°, and west is 270°. The receiving surface can be defined by its orientation (O) and inclination (I). The orientation follows the same rule with the azimuth. For

the inclination, it is equal to 0° for horizontal surfaces and 90° for vertical surfaces.

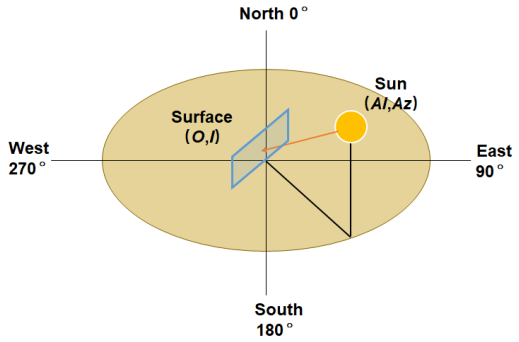

Figure 8 Definition of solar angles and surface angles

The direct incident solar radiation (*S*) can be calculated separately by the following formulae based on the DNSG (*NS*):

$$S = \frac{NS \times timestep \times (\sin(I) \times \cos(Al) \times \cos(I - Az) + \cos(I) \times \sin(Al))}{3600} \quad (5)$$

when $Al > 0$ and $-90° \le I\text{-}Az \le 90°$

Finally, we evaluated the proposed method for direct incident solar radiation by comparing the estimated results with ground truth and the estimated results of the three conventional methods. The normalized mean bias error (NMBE) and the coefficient of variation of the root mean square error (CVRMSE) were used to quantify the differences among the calculation results. The ground truth and various estimated results are at different time intervals (i.e., 1 min, 10 min and 1 hour). To compare the direct incident solar radiation, the ground truth and subhourly estimated results were generated at 1-h interval by aggregating subhourly results within the hour. The NMBE can reflect the calculation accuracy regarding annual direct incident solar radiation, whereas CVRMSE is used to compare the estimated hourly incident radiation profile quantitatively with the hourly aggregations of ground truth. The calculation formulae are as follows:

$$NMBE = \frac{\sum_{i=1}^{n} (y_i - \hat{y}_i)}{n \times \bar{y}} \quad (6)$$

$$CVRMSE = \frac{\left[\sum_{i=1}^{n} \frac{(y_i - \hat{y}_i)^2}{n}\right]^{1/2}}{\bar{y}} \quad (7)$$

where y_i is the ground truth, $\hat{y}_i$ is the estimated value, n is the number of data points used in comparison, and $\bar{y}$ is the average ground truth.

Note that programs follow different conventions to treat timestamp corresponding to hourly solar insolation in the weather file. The solar insolation in the weather file of DOE-2 and EnergyPlus is over the previous timestamp (for Hour 11, it's the total from 10:00-11:00), and the solar insolation in the weather file of DeST is over the present timestamp (for Hour 11, it's the total from 11:00-

12:00). Therefore, this study follows the convention used in DeST to make the results of different programs comparable. Specifically, estimated incident solar radiation is over the present timestamp, for example, hourly incident solar radiation at 11:00 represents the total amount of incident solar radiations from 11:00 to 12:00.

2.5. Sensitivity analysis

BEMPs typically adopt the hourly DNSI (Wh/m^2) as an input. DNSG (W/m^2) should first be estimated under different algorithms, and then used for a direct incident solar radiation calculation. Therefore, the estimation algorithm for irradiance is one of the most important factors in a direct incident solar radiation calculation. In addition, the timestep and time point for the solar position can also impact the estimation results. Different timesteps (e.g., 10 min or 1 h) are usually adopted in the calculation of solar radiation incident on a surface. The direct incident solar radiation value was calculated at each timestep and was regarded as unchanging during each interval. Therefore, the timestep can also impact the estimation results. Because the solar position and irradiance change over time, we should choose a time point for the solar position and irradiance at each timestep when calculating the direct incident solar radiation[47]. In general, we focus on the impact of the estimation algorithm for irradiance, the timestep, and time point for the solar position coupled with the estimation accuracy of direct incident solar radiation. The settings of these factors are shown in Table 3.

Table 3 Settings of factors in the sensitivity analysis

Factors	Settings
Timestep	10 min, and 1 h
Time point for the solar position	The beginning, middle, and end of every timestep
Estimation algorithm for irradiance	0-order interpolation, 1-order interpolation, and saw-tooth algorithm

We still take the calculated direct incident solar radiation on the surfaces from the DNSG as the ground truth, which was used to analyze the impacts of different factors on the estimation accuracy.

3. Results of the case study

We first calculated the direct solar radiation incident on different surfaces based on the DNSG, which was considered as the ground truth. We then estimated the direct incident solar radiation from the hourly DNSI data using the four methods (i.e., methods in DOE-2, EnergyPlus, DeST, and the proposed method). The comparisons between the estimated results with the ground truth are described in the following sections.

3.1. Comparison results of aggregated direct incident solar radiation

The aggregated direct incident solar radiation levels of the four methods for 2016 in different cities are compared in Figure 9. The estimated aggregated direct incident solar radiations of DOE-2, EnergyPlus, and the proposed method were close to the ground truth, the NMBE of which is lower

than 2% in most cases. The proposed method can obtain better results comparatively in terms of the aggregated direct incident solar radiation. Because China is located in the northern hemisphere, north-facing surfaces rarely receive direct solar radiation except for a few hours after sunrise and before sunset, resulting in large estimation errors in such surfaces. However, the DeST method overestimated the aggregated direct solar radiation on the east-facing surfaces by 14%–30% and underestimated the aggregated direct solar radiation on the west-facing surfaces by 16%–21%.

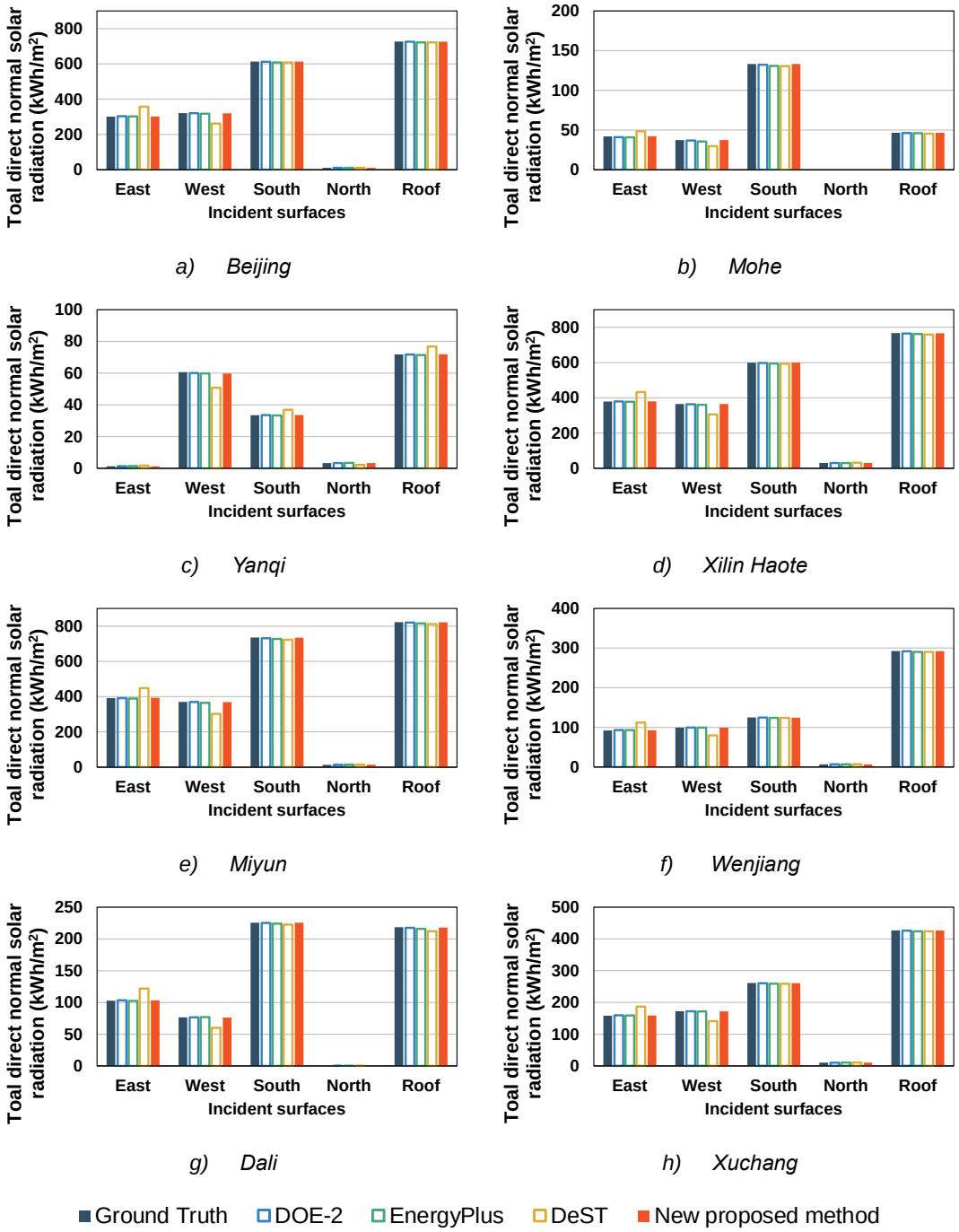

Figure 9 Aggregated direct solar radiation on different surfaces in eight stations in 2016

3.2. Comparison results on hourly direct incident solar radiation

Taking the estimated results of hourly direct incident solar radiation on August 22, 2016 in Beijing as an example (Figure 10), the estimated hourly direct incident radiation by DeST significantly differs from the ground truth. For instance, the estimated hourly direct radiation on the east-facing surface is much higher than the ground truth, whereas the DOE-2 can achieve a more accurate estimation of the hourly direct incident solar radiation. The only difference between the methods in DOE-2 and DeST is the time point for the solar position, which means that remarkable errors may occur when applying the beginning of every timestep for the solar position. There are some differences between the estimated results using the EnergyPlus method with the ground truth, particularly at sunrise. As shown in Figure 10, the hourly direct solar radiation on the east- and north-facing surfaces by EnergyPlus is much higher at 5:00. The proposed method also obtains better results in terms of the hourly results.

To compare the hourly results in different cities and during a long period of time, we show the CVRMSEs of the hourly results on different surfaces by applying the four methods for the eight cities in Figure 11. The accuracies of the four methods in terms of the estimated hourly direct incident solar radiation are ranked in the following order: proposed method, DOE-2, EnergyPlus, and DeST.

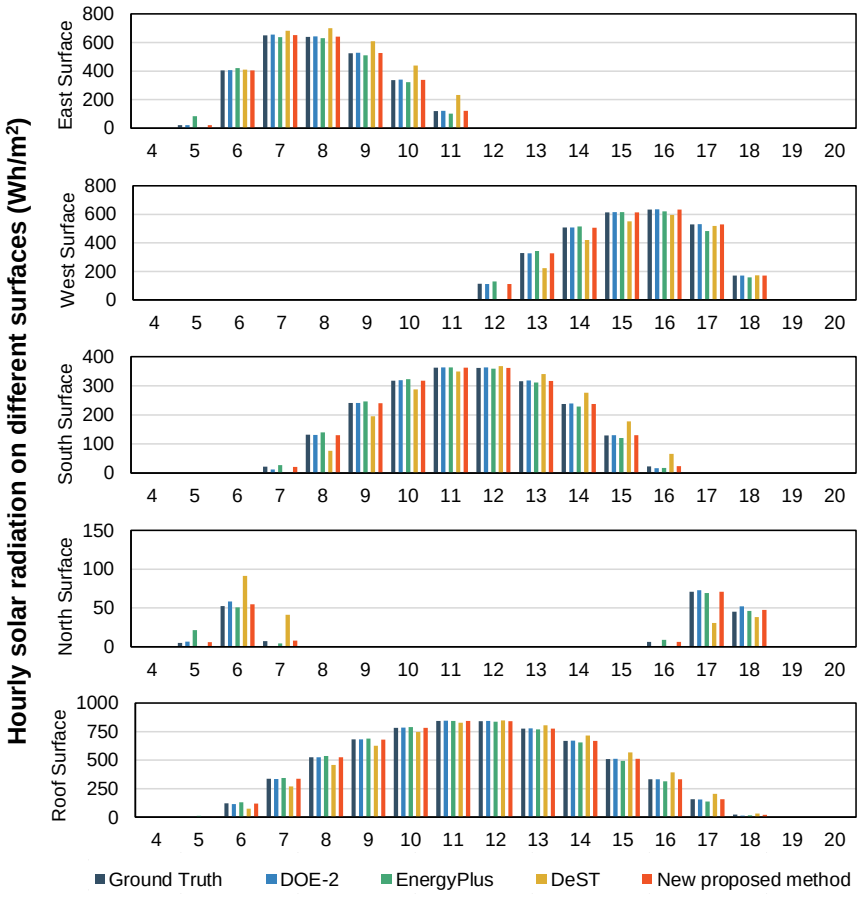

Figure 10 Hourly direct solar radiation on different surfaces on August 26, 2016 in Beijing

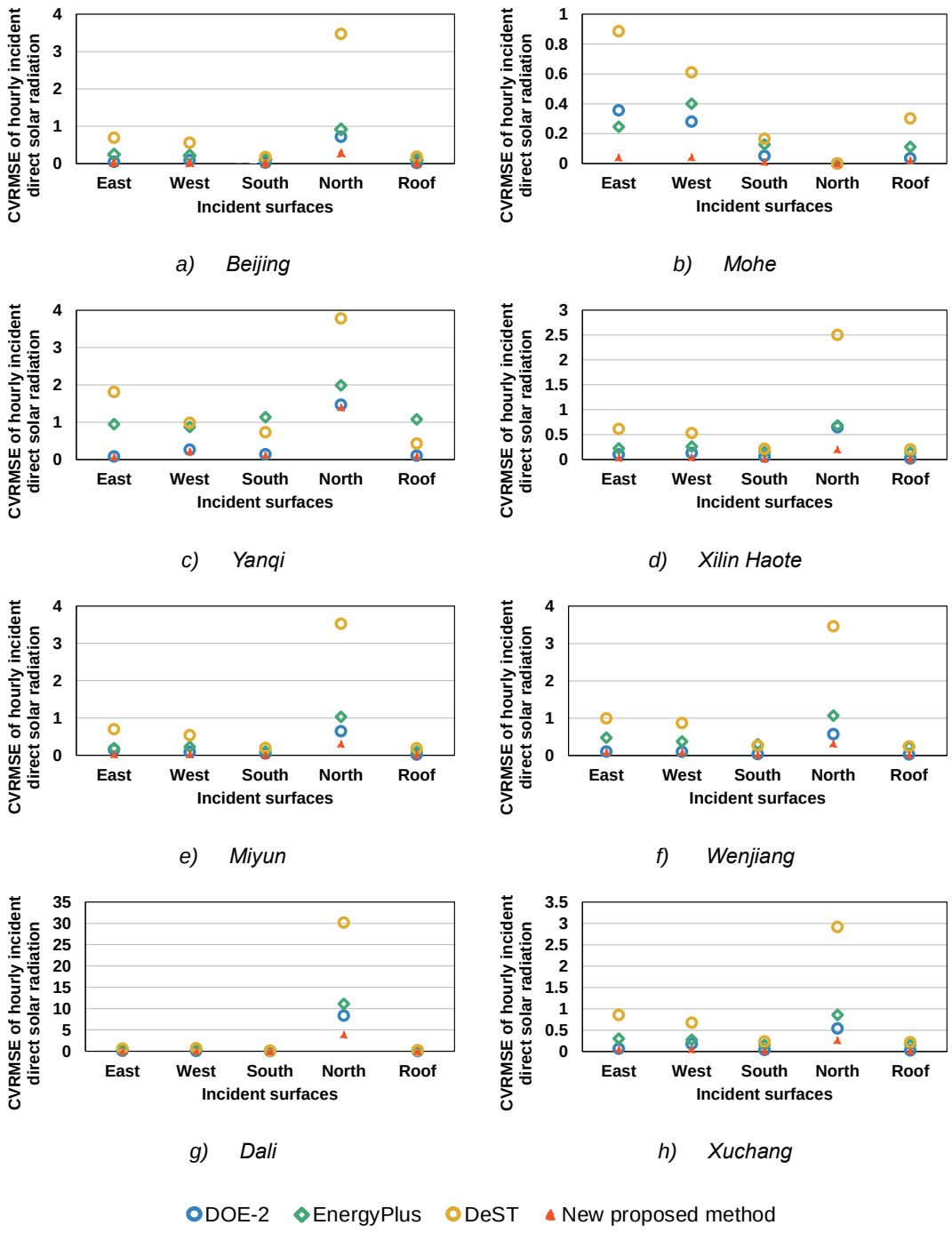

Figure 11 CVRMSE of hourly direct solar radiation on different surfaces in eight stations in 2016

3.3. Comparison results on direct incident solar radiation in minutes

Diurnal variation curves of incident solar irradiance in minutes were compiled from the ground truth and the four calculation methods and are shown in Figure 12 (the three vertical lines in figures represent sunrise, solar noon and sunset from left to right). It can be observed that DOE-2 and DeST, which adopt zero-order interpolation for a solar irradiance estimation, cannot reflect the change in solar radiation within a 1-h period. The variation curves of the results estimated using EnergyPlus and the proposed approach are much closer to the ground truth owing to the linear assumption of the solar

irradiance. However, some differences remain between the estimation by EnergyPlus and the ground truth. For instance, as shown in Figure 13, the estimated solar irradiances on the east-facing surface by EnergyPlus are much higher between 5:00 and 6:00, whereas the proposed method performs much better in terms of direct incident solar radiation in minutes.

In addition, Figure 14 shows diurnal variation curves of incident solar irradiance in minutes of estimations and ground truth on a cloudy day. It indicates that owning to the randomness of solar irradiances on cloudy days, all these methods cannot predict solar irradiance on cloudy days very well.

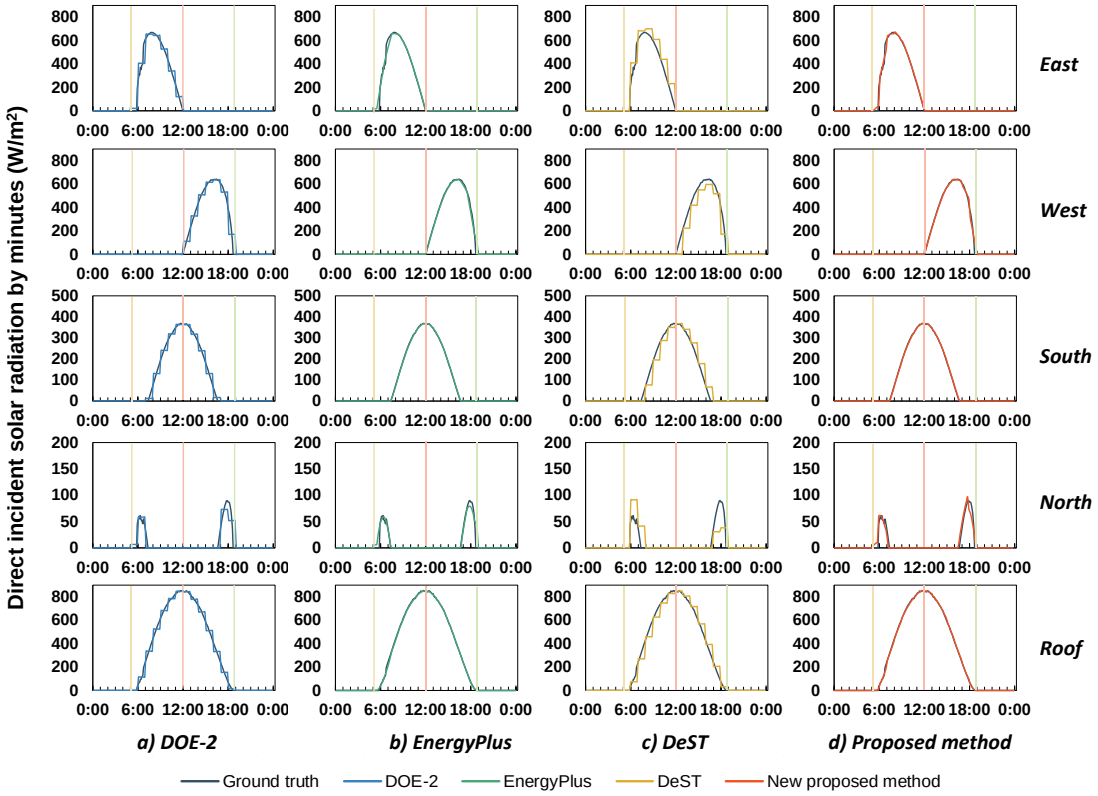

Figure 12 Solar radiation in minutes on different surfaces on August 26, 2016 in Beijing

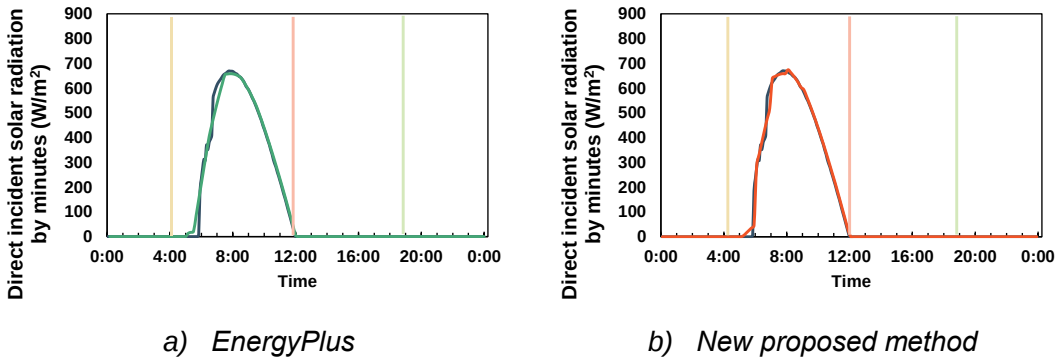

Figure 13 Solar radiation in minutes on the east-facing surface on August 26, 2016 in Beijing

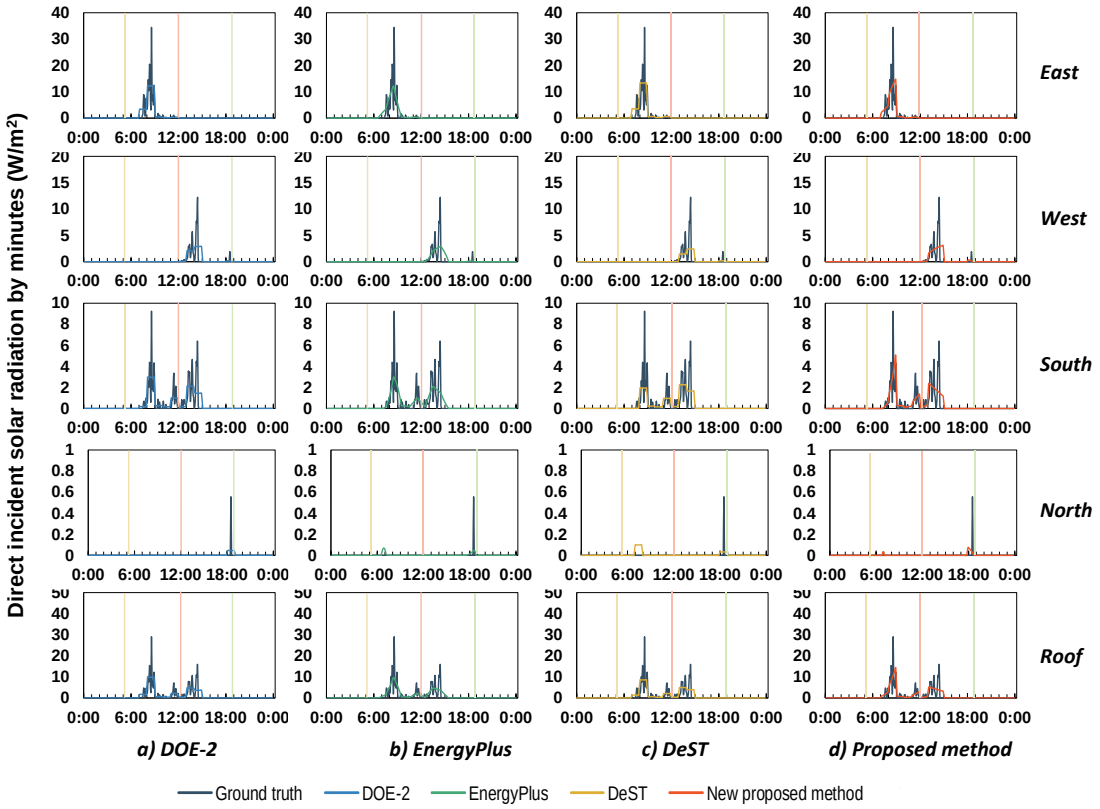

Figure 14 Solar radiation in minutes on different surfaces on September 1, 2016 in Beijing

4. Sensitivity analysis of different factors

During the comparison of the four methods on the calculation of direct incident solar radiation, we found that the estimation algorithm for irradiance, the timestep, and the time point for the solar position are extremely important factors for a direct incident solar radiation calculation. Therefore, we will discuss the impacts of these three factors on the estimation accuracy of direct incident solar radiation using Beijing as an example.

4.1. Influence of time point for the solar position

When calculating the direct incident solar radiation, the direct incident solar radiation value is calculated at each timestep and is regarded as unchanging during each interval, so we should choose a time point for the solar position and irradiance at each timestep. Different time points represent different solar positions at each timestep for calculation, for which corresponding different incident angles will be used when converting the DNSG can into the incident radiation on a tilted surface.

We calculated the direct solar radiation incident on the surfaces using different time points for the solar position (i.e., beginning, middle, and end of every timestep). These three methods adopted 1 h as the timestep and zero-order interpolation for the irradiance estimation. The aggregated direct incident solar radiation during 360 days for the ground truth and the estimated results are shown in Figure 15. As the figure indicates, the estimated aggregated direct incident solar radiation is quite close to the ground truth (i.e., less than 3%) when using the middle of every timestep for the solar

position; however, when using the beginning of every timestep, the estimated result incident on the east surface is much higher than the ground truth (i.e., 18.8%), the estimation for the west surface is obviously lower than that of the ground truth (i.e., 18.3%), and the estimations for the remaining three surfaces are almost the same. In addition, when using the end of every timestep, the bias of the estimated results shows the opposite tendency with that using the beginning as the time point.

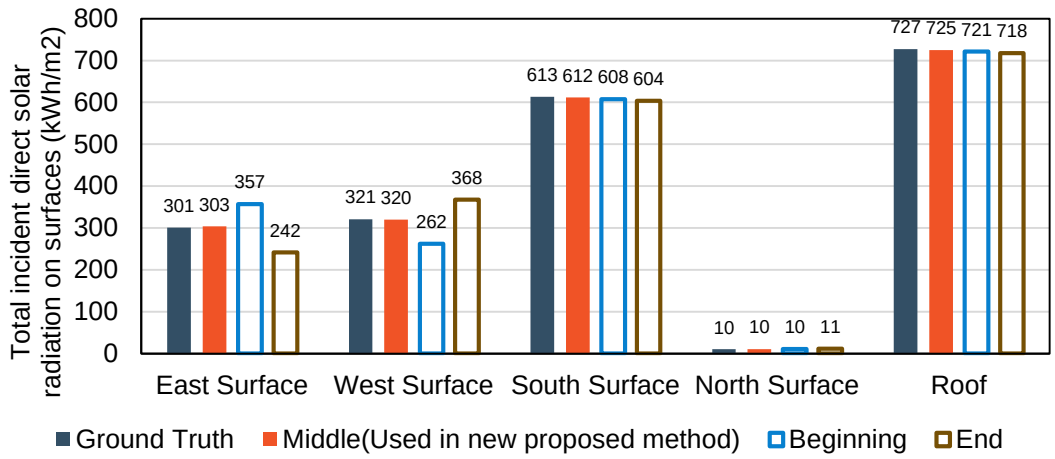

Figure 15 Aggregated direct solar radiation on surfaces for the ground truth and estimations using different time points for the solar position

We compared the diurnal variation curves of the hourly direct solar radiation incident on different surfaces for the methods with different time points regarding the solar position with the ground truth on a typical summer day, as shown in Figure 16. When using the beginning of the timestep, the estimated direct incident radiation significantly differs from ground truth, i.e., it is higher on the east-facing surface, lower on the west-facing surface, higher in the morning and lower in the afternoon on the north-facing surface, and lower in the morning and higher in the afternoon on the south-facing and roof surfaces. The use of the end of every timestep shows an opposite result as the beginning. This is mainly caused by different incident angles corresponding to different time points. The incident angle corresponding to the middle of every timestep is very close to the average incident angles during one timestep, whereas the another two types of time points use the incident angles with significant differences for calculation.

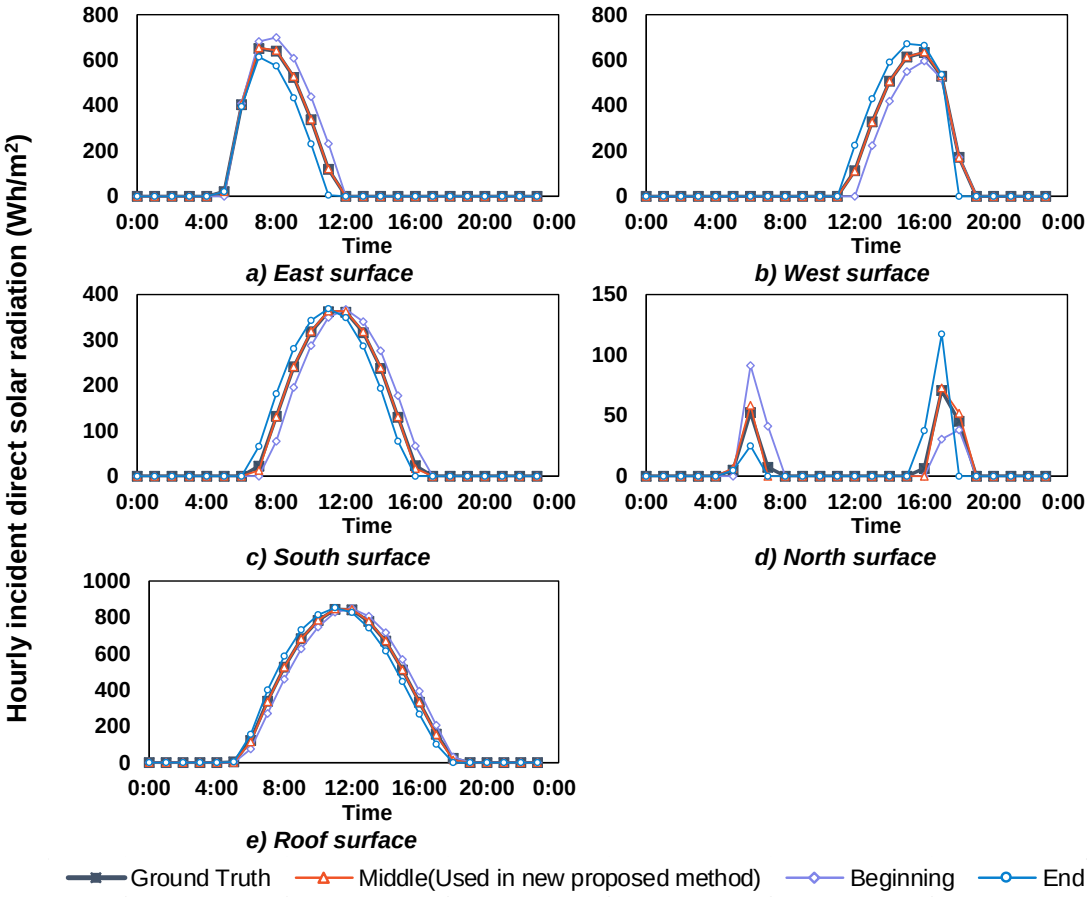

Figure 16 Hourly direct solar radiation incident on surfaces on August 26, 2016 for the ground truth and estimations using different time points for the solar position

4.2. Influence of timestep

We compared the estimated direct solar radiation incident on the surfaces using two different timesteps (i.e., 10 min and 1 h) with the ground truth. These methods adopted zero-order interpolation for the solar irradiance estimation. As shown in Figure 17, methods with small timesteps have smaller differences with the ground truth in terms of the aggregated direct incident solar radiation. For methods using the beginning of the timestep, the error rate decreased significantly with the decrease in the timestep, whereas the difference in the aggregated direct incident radiation between the two timesteps is not as obvious when using the middle of the timestep.

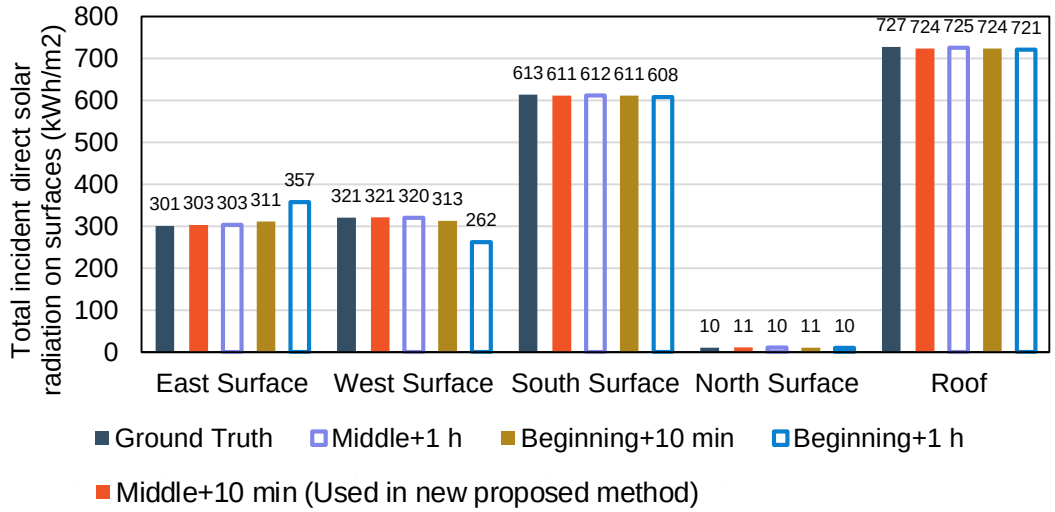

Figure 17 Aggregated direct solar radiation on surfaces of the ground truth and estimations using different timesteps

We also present the diurnal variation curves of the hourly estimations and the ground truth of direct solar radiation incident on the surfaces and ground truth in Figure 18. It can be concluded that a smaller timestep can lead to a smaller error rate. The error rate is relatively clear when using 1 h as the timestep. For methods applying the beginning of the timestep, using a 1-h timestep results in remarkable errors during the period of 12:00–15:00 as compared with that using 10 min as the timestep. For the method applying the middle of the timestep, the estimated incident radiation at 19:00 when using a 1-h timestep is lower than the ground truth.

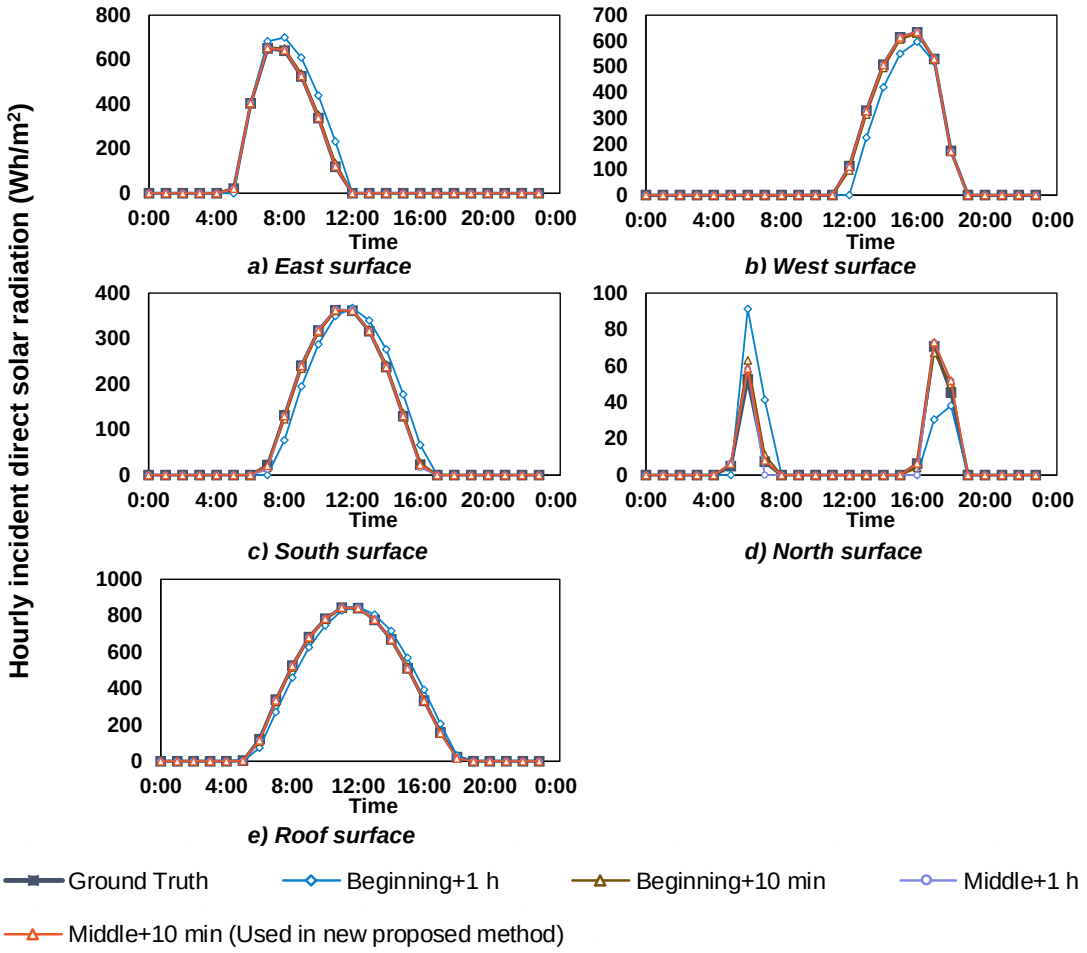

Figure 18 Hourly direct solar radiation incident on surfaces on August 26, 2016 for the ground truth and estimations using different timesteps

4.3. Influence of estimation algorithms for irradiance

We compared the direct solar radiation incident on the surfaces for the ground truth and estimations using different estimation algorithms for the solar irradiance from three dimensions, namely, the annual amount of incident radiation, the diurnal variation curve of hourly direct incident solar radiation, and direct incident solar radiation in minutes. Note that the 10-min timestep and the middle of every timestep for the solar position were adopted for estimations. As shown in Figure 19, the aggregated direct solar radiation incident on the surfaces when using the different estimation algorithms is quite close to the ground truth. However, for the diurnal vitiation curves of the hourly results shown in Figure 20, we found that some differences exist when using the first-order interpolation because this method cannot guarantee that the hourly solar radiation will remain constant after estimating solar irradiance. Although zero-order interpolation and the proposed saw-tooth algorithm can both obtain good estimations of the hourly results, in terms of the estimated direct incident solar radiation in minutes shown in Figure 21, the proposed saw-tooth algorithm performs much better. The zero-order interpolation method assumes that the solar irradiance is constant during a 1-h period, whereas the proposed saw-tooth algorithm can reflect the variation in the solar irradiance within 1 h. However, this algorithm also has two disadvantages: 1) it cannot reflect a rapid change in the solar irradiance in 1 h

owing to the movement of the clouds, and 2) solar irradiance occurring at the end of the last hour may not be equal to the data at the beginning of the present hour. In general, the proposed saw-tooth algorithm achieves a better performance.

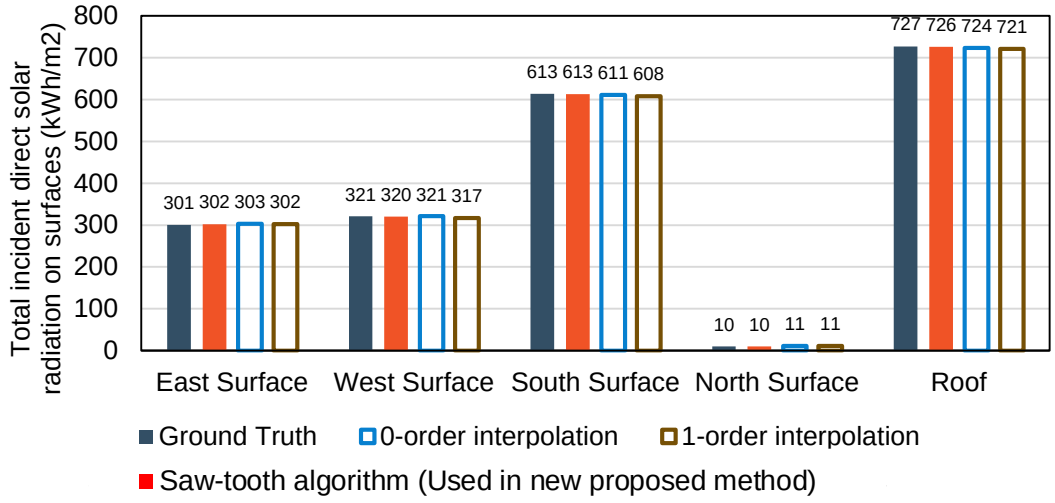

Figure 19 Aggregated direct solar radiation incident on surfaces for ground truth and estimations using different estimation algorithms for solar irradiance

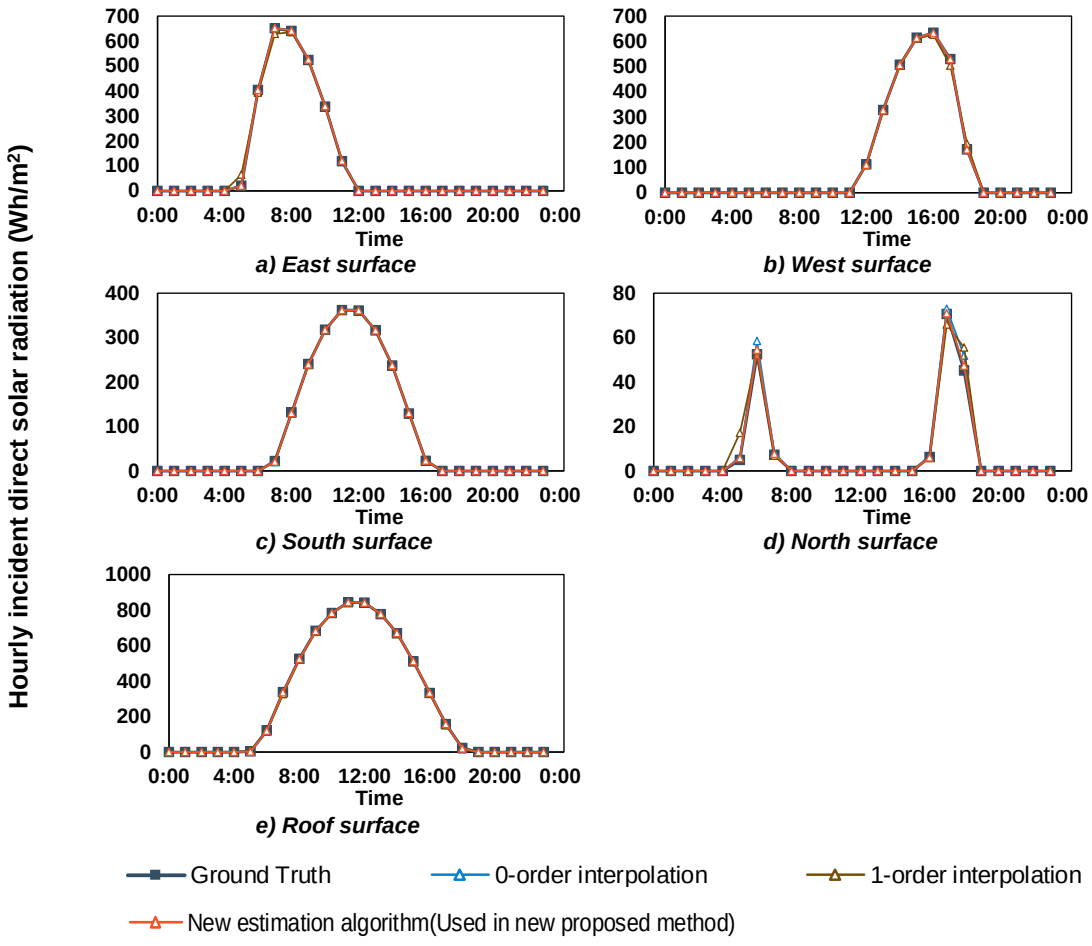

Figure 20 Hourly direct normal solar radiation incident on the surfaces on August 26, 2016 for the ground truth and estimations using different estimation methods for the solar irradiance

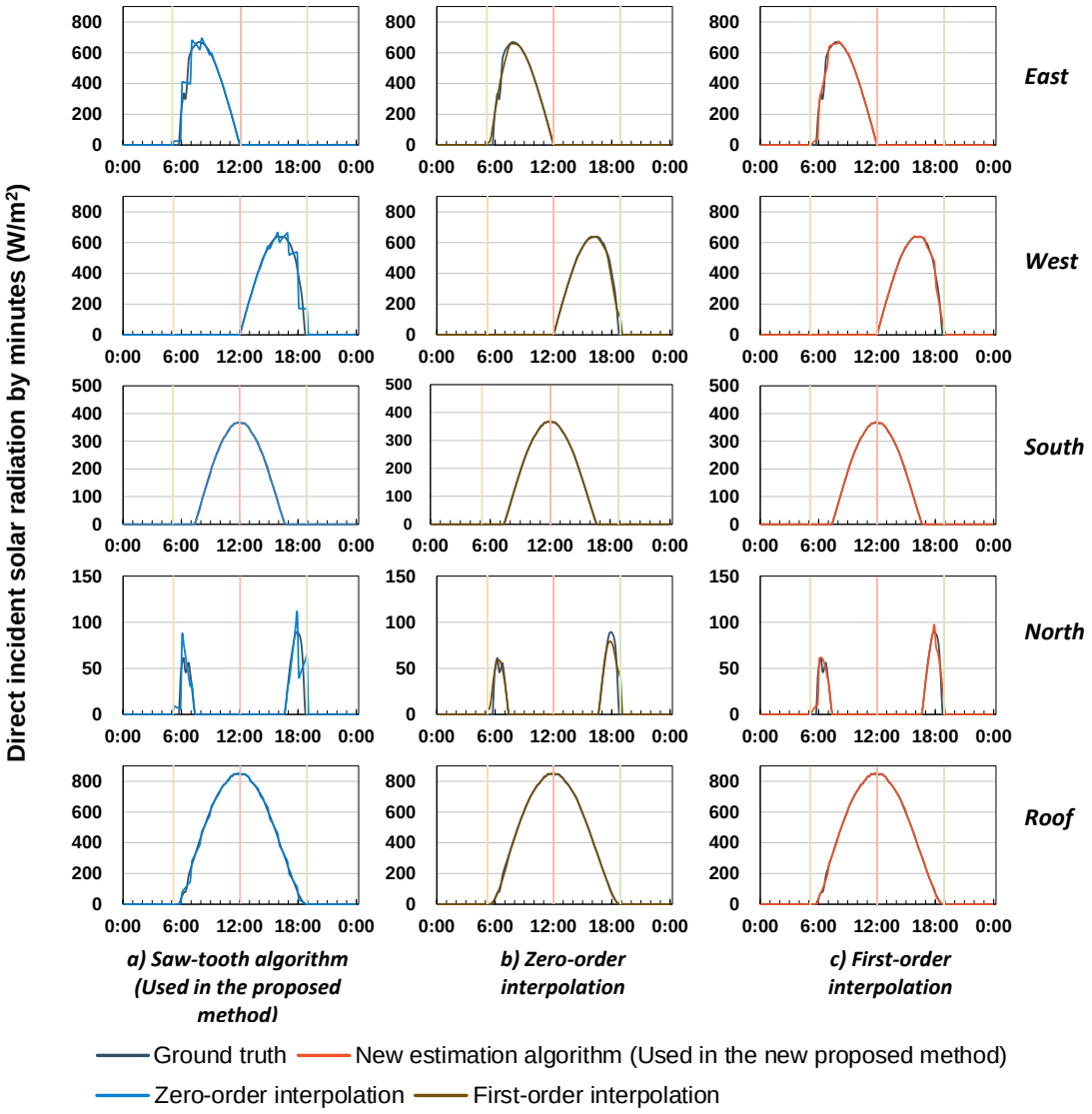

Figure 21 DNSG in minutes incident on the surfaces on August 26, 2016 for the ground truth and estimations using different estimation methods for the solar irradiance

5. Conclusion

Solar radiation on a surface significantly impacts the energy consumption of buildings and the power generation of BIPV systems. Hourly solar insolation (Wh/m^2) is the most common input for incident solar radiation calculations in BEMPs. Therefore, the DNSG (W/m^2) should be estimated first, followed by calculations of the direct solar radiation incident on surfaces with different angles according to the geometrical relationship. However, this calculation process might cause a difference between the estimations and the actual direct incident solar radiation.

Based on a comparative analysis of three conventional methods used in BEMPs (i.e., DOE-2,

EnergyPlus, and DeST), in this study, an improved method for calculating the direct incident solar radiation on exterior building surfaces was proposed. The proposed method applies a new algorithm for an irradiance estimation, together with a 10-min timestep and the use of the middle of every timestep for the solar position. The new algorithm applied for an irradiance estimation assumes that the solar irradiance changes linearly within a 1-h period, and the slope is estimated based on the solar insolation values during the last hour, the present hour, and the next hour.

The comparison results for 2016 in eight cities in China indicate that the three conventional methods have certain issues: The DeST obtains a poor estimation because it adopts the beginning of the timestep for the solar position. The hourly incident radiation estimated by EnergyPlus differs from the actual value because its estimation algorithm for irradiance cannot keep the hourly solar insolation constant after an estimation of the solar irradiance. Finally, the DOE-2 is relatively good, but it regards the solar irradiance as remaining constant within 1 h, and thus there are obvious differences between the estimated results and the actual results when considering the incident solar irradiance in minutes. The proposed method has significant advantages in contrast to the three conventional methods used in the BEMPs. It can also guarantee that the hourly direct solar insolation stays the same as in the weather file and reflects the variation in the direct solar irradiance across the hour. However, both existing methods in BEMPs and this proposed method cannot accurately predict solar irradiance on cloudy days. The solar irradiances on cloudy days have strong randomness, but all these methods are to smooth the solar irradiance profile and make it continuous. Better solutions for solar irradiance calculation on cloudy days can be studied in the future.

This study further discussed the impact of the time point for the solar position, timestep, and algorithm for irradiance on the estimation accuracy of the direct incident solar radiation using Beijing as an example. The proposed method obtains more accurate results when using the middle point of every timestep and by applying a short timestep (i.e., 10 min), which can be adopted in current BEMPs to improve the accuracy of a simulated building performance and BIPV production. However, this study focuses on the comparison and analysis of calculation methods and lacks quantitative calculation of impacts of different calculation methods on estimated building energy consumption or BIPV production, which can be studied in the future.

Acknowledgment

This study was supported by “the 13th Five-Year” National Science and Technology Major Project of China (No. 2018YFC0704500), Beijing Municipal Natural Science Foundation of China (grant number 8182026), and Beijing Advanced Innovation Center for Future Urban Design, Beijing University of Civil Engineering And Architecture. The authors appreciate Jingjin Ma for his kind help of this study.

Reference

[1] F. Causone, S.P. Corgnati, M. Filippi, B.W. Olesen, Solar radiation and cooling load calculation for radiant systems: Definition and evaluation of the Direct Solar Load, Energy Build. 42 (2010) 305–314. https://doi.org/10.1016/j.enbuild.2009.09.008.

[2] S. Pal, B. Roy, S. Neogi, Heat transfer modelling on windows and glazing under the exposure of solar radiation, Energy Build. 41 (2009) 654–661. https://doi.org/10.1016/j.enbuild.2009.01.003.

[3] F.J.S. de la Flor, R.O. Cebolla, J.L.M. Félix, S.Á. Domínguez, Solar radiation calculation methodology for building exterior surfaces, Sol. Energy. 79 (2005) 513–522.

[4] U.S. DOE, Windows and building envelope research and development: roadmap for emerging technologies, 2014.

[5] B. Chen, Y. Ji, P. Xu, Impact of window shading devices on energy performance of prototypical buildings, in: Asim 2012, Tongji University, Shanghai, China, 2012.

[6] R. Yin, P. Xu, P. Shen, Case study: Energy savings from solar window film in two commercial buildings in Shanghai, Energy Build. 45 (2012) 132–140. https://doi.org/10.1016/j.enbuild.2011.10.062.

[7] C.A. Hviid, T.R. Nielsen, S. Svendsen, Simple tool to evaluate the impact of daylight on building energy consumption, Sol. Energy. 82 (2008) 787–798. https://doi.org/10.1016/j.solener.2008.03.001.

[8] R. V. Ralegaonkar, R. Gupta, Review of intelligent building construction: A passive solar architecture approach, Renew. Sustain. Energy Rev. 14 (2010) 2238–2242. https://doi.org/10.1016/j.rser.2010.04.016.

[9] B. Parida, S. Iniyan, R. Goic, A review of solar photovoltaic technologies, Renew. Sustain. Energy Rev. 15 (2011) 1625–1636. https://doi.org/10.1016/j.rser.2010.11.032.

[10] C. Peng, Y. Huang, Z. Wu, Building-integrated photovoltaics (BIPV) in architectural design in China, Energy Build. 43 (2011) 3592–3598. https://doi.org/10.1016/j.enbuild.2011.09.032.

[11] H.Y. Cheng, C.C. Yu, K.C. Hsu, C.C. Chan, M.H. Tseng, C.L. Lin, Estimating solar irradiance on tilted surface with arbitrary orientations and tilt angles, Energies. 12 (2019) 1–14. https://doi.org/10.3390/en12081427.

[12] A.K. Yadav, S.S. Chandel, Tilt angle optimization to maximize incident solar radiation: A review, Renew. Sustain. Energy Rev. 23 (2013) 503–513. https://doi.org/10.1016/j.rser.2013.02.027.

[13] C. Demain, M. Journée, C. Bertrand, Evaluation of different models to estimate the global solar radiation on inclined surfaces, Renew. Energy. 50 (2013) 710–721. https://doi.org/10.1016/j.renene.2012.07.031.

[14] A.G. Slater, Surface solar radiation in North America: A comparison of observations, reanalyses, satellite, and derived products, J. Hydrometeorol. 17 (2016) 401–420.

[15] K.H. Kim, J. Kie-Whan Oh, W.S. Jeong, Study on solar radiation models in South Korea for improving office building energy performance analysis, Sustain. 8 (2016). https://doi.org/10.3390/su8060589.

[16] X.L. Ren, H.L. He, L. Zhang, L. Zhou, G.R. Yu, J.W. Fan, Spatiotemporal variability analysis

of diffuse radiation in China during 1981-2010, Ann. Geophys. 31 (2013) 277–289. https://doi.org/10.5194/angeo-31-277-2013.

[17] J.L. Chen, G.S. Li, Estimation of monthly average daily solar radiation from measured meteorological data in Yangtze River Basin in China, Int. J. Climatol. 33 (2013) 487–498. https://doi.org/10.1002/joc.3442.

[18] S. Janjai, P. Pankaew, J. Laksanaboonsong, P. Kitichantaropas, Estimation of solar radiation over Cambodia from long-term satellite data, Renew. Energy. 36 (2011) 1214–1220. https://doi.org/10.1016/j.renene.2010.09.023.

[19] F. Kasten, G. Czeplak, Solar and terrestrial radiation dependent on the amount and type of cloud, Sol. Energy. 24 (1980) 177–189. https://doi.org/10.1016/0038-092X(80)90391-6.

[20] Z. Qingyuan, J. Huang, L. Siwei, Development of typical year weather data for Chinese locations, ASHRAE Trans. 108 (2002) 1063–1075.

[21] H.D. Kambezidis, B.E. Psiloglou, The meteorological radiation model (MRM): Advancements and applications, Model. Sol. Radiat. Earth's Surf. Recent Adv. (2008) 357–392. https://doi.org/10.1007/978-3-540-77455-6_14.

[22] M. Wild, E. Schmucki, Assessment of global dimming and brightening in IPCC-AR4/CMIP3 models and ERA40, Clim. Dyn. 37 (2011) 1671–1688. https://doi.org/10.1007/s00382-010-0939-3.

[23] J. Huang, M. Korolkiewicz, M. Agrawal, J. Boland, Forecasting solar radiation on an hourly time scale using a Coupled AutoRegressive and Dynamical System (CARDS) model, Sol. Energy. 87 (2013) 136–149. https://doi.org/10.1016/j.solener.2012.10.012.

[24] A.K. Yadav, S.S. Chandel, Solar radiation prediction using Artificial Neural Network techniques: A review, Renew. Sustain. Energy Rev. 33 (2014) 772–781. https://doi.org/10.1016/j.rser.2013.08.055.

[25] R.C. Deo, X. Wen, F. Qi, A wavelet-coupled support vector machine model for forecasting global incident solar radiation using limited meteorological dataset, Appl. Energy. 168 (2016) 568–593. https://doi.org/10.1016/j.apenergy.2016.01.130.

[26] A. Ben Othman, K. Belkilani, M. Besbes, Global solar radiation on tilted surfaces in Tunisia: Measurement, estimation and gained energy assessments, Energy Reports. 4 (2018) 101–109. https://doi.org/10.1016/j.egyr.2017.10.003.

[27] A. Sanchez-Lorenzo, J. Calbó, M. Wild, Global and diffuse solar radiation in Spain: Building a homogeneous dataset and assessing their trends, Glob. Planet. Change. 100 (2013) 343–352. https://doi.org/10.1016/j.gloplacha.2012.11.010.

[28] A. Molina, M. Falvey, R. Rondanelli, A solar radiation database for Chile, Sci. Rep. 7 (2017) 1–11. https://doi.org/10.1038/s41598-017-13761-x.

[29] M. Sengupta, Y. Xie, A. Lopez, A. Habte, G. Maclaurin, J. Shelby, The National Solar Radiation Data Base (NSRDB), Renew. Sustain. Energy Rev. 89 (2018) 51–60. https://doi.org/10.1016/j.rser.2018.03.003.

[30] P. Denholm, R.M. Margolis, Land-use requirements and the per-capita solar footprint for photovoltaic generation in the United States, Energy Policy. 36 (2008) 3531–3543.

[31] S. Wilcox, W. Marion, Users manual for TMY3 data sets, National Renewable Energy Laboratory Golden, CO, 2008.

[32] M. Herrera, S. Natarajan, D.A. Coley, T. Kershaw, A.P. Ramallo-González, M. Eames, D. Fosas, M. Wood, A review of current and future weather data for building simulation, Build. Serv. Eng. Res. Technol. 38 (2017) 602–627. https://doi.org/10.1177/0143624417705937.

[33] Y. Joe, H. Fenxian, D. Seo, M. Krarti, Development of 3012 IWEC2 Weather Files for International Locations (RP-1477)., Ashrae Trans. 120 (2014).

[34] D.J. Thevenard, A.P. Brunger, The development of typical weather years for international locations: part I, algorithms, Ashrae Trans. 108 (2002) 376.

[35] ASHRAE, International Weather for Energy Calculations, V2.0 User Manual and DVD, (2011).

[36] M.E. Eames, A.P. Ramallo-Gonzalez, M.J. Wood, An update of the UK's test reference year: The implications of a revised climate on building design, Build. Serv. Eng. Res. Technol. 37 (2016) 316–333.

[37] Climate Information Center in China Meteorological Bureau, Department of Building Science and Technology in Tsinghua Univerisity, China Standard Weather Data for Analyzing Building Thermal Conditions, China Architecture and Building Press, Beijing, 2015.

[38] R.D. García, E. Cuevas, R. Ramos, V.E. Cachorro, A. Redondas, J.A. Moreno-Ruiz, Description of the Baseline Surface Radiation Network (BSRN) station at the Izaña Observatory (2009–2017): Measurements and quality control/assurance procedures, Geosci. Instrumentation, Methods Data Syst. 8 (2019) 77–96.

[39] D.A. York, C.C. Cappiello, K.H. Olson, DOE-2 Reference Manual: Version 2.1 C, Los Alamos National Laboratory, Solar Energy Group, 1984.

[40] D. Yan, J. Xia, W. Tang, F. Song, X. Zhang, Y. Jiang, DeST --- An integrated building simulation toolkit Part I: Fundamentals, Build. Simul. 1 (2008) 95–110. https://doi.org/10.1007/s12273-008-8118-8.

[41] D.B. Crawley, L.K. Lawrie, F.C. Winkelmann, W.F. Buhl, Y.J. Huang, C.O. Pedersen, R.K. Strand, R.J. Liesen, D.E. Fisher, M.J. Witte, J. Glazer, EnergyPlus: Creating a new-generation building energy simulation program, Energy Build. 33 (2001) 319–331. https://doi.org/10.1016/S0378-7788(00)00114-6.

[42] T.P. McDowell, M. Kummert, Estimating sub-hourly solar radiation and effective sky temperature from hourly weather data, in: Proc. ASHRAE IBPSA-USA SimBuild 2016 Build. Perform. Model. Conf., Salt Lake City, 2016.

[43] W.D. Lubitz, Effect of manual tilt adjustments on incident irradiance on fixed and tracking solar panels, Appl. Energy. 88 (2011) 1710–1719. https://doi.org/10.1016/j.apenergy.2010.11.008.

[44] D. Zhu, T. Hong, D. Yan, C. Wang, Comparison of building energy modeling programs: building loads, U.S. Department of Energy, 2012.

[45] T. McDowell, S. Letellier-Duchesne, M. Kummert, Methods for Determining Sub-hourly Solar Radiation from Hourly Data, in: Proc. ASHRAE IBPSA-USA SimBuild 2018 Build. Perform. Model. Conf., Chicago, 2018.

[46] The Math Work, Inc., MATLAB, Version R2018b, (2018). https://www.mathworks.com/.

[47] I.R. Maestre, J.L.F. Blázquez, F.J.G. Gallero, P.R. Cubillas, Influence of selected solar positions for shading device calculations in building energy performance simulations, Energy Build. 101 (2015) 144–152. https://doi.org/10.1016/j.enbuild.2015.05.004.